Typeset using LaTeX **manuscript** style in AASTeX631

Applying the Method of Gauss to Determine the Orbit of Asteroid A910 LC

Agrawal, D., Pramanik, S., Zhang, J.[1]

[1]*Summer Science Program and Pohl Observatory, Georgia College and State University, Milledgeville, GA, 31061, USA*

(Received August 20, 2024)

ABSTRACT

There are thousands of asteroids in the solar system that have orbits that cross near Earth and Mars. This study determined the orbit of the Mars Crossing Asteroid A910 LC using Gauss's Method. Three observations were taken, two from Pohl Observatory at Georgia College and State University and one from Cerro Tololo Inter-American Observatory in Chile. Flats and darks were taken and applied to images to correct for noise and imperfections in the telescope apparatus. After the position of the asteroid within the image was determined, the Right Ascension (RA) and Declination (DEC) were obtained using Least-Squares Plate Reduction and the USNO-B Catalog. This process found mean RA and DEC values as well as a confidence interval for them. Gauss's Method was then applied to these RA and DEC values, under a convergence interval of 10^{-10}, to find the orbital elements for the asteroid. After, a Monte-Carlo simulation was employed to find the SDOM values for each orbital element for the asteroid. Ultimately, the values found were $a = 2.5995 \pm 0.005$ au, $e = 0.4056 \pm 0.0004$, $i = 15.344 \pm 0.008°$, $\Omega = 242.492 \pm 0.002°$, $\omega = 91.76 \pm 0.06°$, $\nu = 272.31 \pm 0.06°$. The calculated values were off by less than 1% from JPL Horizons' Ephemeris values, which were well within the SDOM for the elements. Sources of error included telescope wobble, which contributed to a larger deviation for the Monte-Carlo simulation, and variation in gaps between times of observation.

1. INTRODUCTION

The solar system is filled with millions of extraterrestrial objects, each following different paths governed by the laws of gravity. Some of these are comets, destined to meet the Sun for a brief moment before spending most of their lives in deep space. Most are asteroids, ranging in size from pebbles to structures a thousand kilometers across, orbiting the sun endlessly in ellipses and circles. Most asteroids live in the Asteroid Belt, which resides between the orbits of Mars and Jupiter. Others orbit in the Kuiper belt outside of Neptune. Some asteroids, however, have elliptical orbits that pass close to the orbits of Earth and Mars, creatively named Near Earth Asteroids and Mars Crossing Asteroids respectively. Near Earth Asteroids have a semimajor axis under 1.3 AU and are further split into four categories based on their semimajor axis and perihelion distance. Atira asteroids are always within Earth's orbit, while Amor asteroids are always exterior to Earth's orbit. Atens and Apollo asteroids are Earth Crossing, meaning at some point, their distance from the sun is 1 AU. Atens asteroids have a semimajor axis under 1 AU, meaning they spend most of their time inside of Earth's orbit, but Apollo asteroids spend most of their time outside of it. Near Mars Asteroids and Mars Crossing Asteroids are defined similarly. Search campaigns like the International Astronomical Search Collaboration involve hundreds and thousands of teams from all around the world, each focusing on detecting and discovering new asteroids. Learning more about these asteroids provides hints to the history of the solar system and helps reduce the chance of a future collision with one of them (1).

This study investigated the Mars Crossing Asteroid A910 LC, nicknamed Hela. This asteroid and all others have six degrees of freedom that define its movement, each for one dimension of position and velocity. Although these degrees of freedom could be described using position and momentum vectors, it is more elegant to describe them using 6 orbital elements. The first two, the semi-major axis a and the eccentricity e, describe the shape of the elliptical orbit. The semi-major axis describes the size of the orbit and the eccentricity describes how elliptical it is, with 0 being a perfect circle and 1 being a degenerate ellipse–a line segment. The true anomaly ν describes the angle of the asteroid along the elliptical orbit with respect to the sun and the asteroid's location at perihelion.

The argument of perihelion ω describes the angle between the perihelion (the closest approach of the asteroid) and the line of nodes, where the asteroid crosses the ecliptic plane. The longitude of the line of nodes Ω describes the angle between the line of nodes and the vernal equinox of Earth's orbit. The inclination i describes the angle between the orbital plane of the asteroid and the ecliptic plane – the orbital plane of the Earth. Together, these 6 orbital elements completely determine the entire motion of the asteroid through its past and future, assuming a simplistic model of the solar system where the Sun is the only source of gravity.

Gauss's method was employed to determine the 6 orbital elements from the observations. Three observations, roughly equally spaced in time, were taken and analyzed to determine the Right Ascension (RA) and Declination (DEC) of the asteroid (3). From there, Gauss's method is applied: an algorithm is used which converges on the values for the orbital elements. A Monte-Carlo simulation is also run to predict all probable paths for the asteroid by adding uncertainty to the RA and DEC values measured based on their standard deviation. This provides a sense of the confidence in the orbital elements obtained. In the end, these elements are used to predict the asteroid's position at future times to see if and when it will intersect Mars' orbital path.

2. OBSERVATIONS AND IMAGE PROCESSING

2.1. *Data Acquisition*

To determine the orbit of the asteroid, three observations were conducted. The first two observations were made at the Pohl Observatory in Georgia, USA. The final observation utilized the online telescope at the Cerro Tololo Inter-American Observatory in Chile. The following two tables show the essential information for both telescopes and the observations.

Table 1: Observatory Features

Features	GC Observatory	CTIA Observatory
Aperture	0.61 m	0.4 m
Focal Length	3974 mm	4576.0 mm
F-ratio	6.5	11.3
CCD Size	3326 × 2504	1024 × 1024
FOV	14.0 × 14.0 arcmin	10.0 × 10.0 arcmin

Table 2: Observational Journal

Date	Time (UTC)	Location	Sets Taken	Exposure/Image (s)	Images/Sequence
06/20/24	02:10-02:30	GC Observatory	3	8	7
06/24/24	03:10-03:30	GC Observatory	3	10	7
07/03/24	23:27-23:47	CTIA Observatory	2	64.52	1

During the observations at the Pohl Observatory, TheSkyX software was used to control all equipment, including the telescope, dome, camera, and filter wheel. TheSkyX was then connected to SiTech, which manages the telescope's motion. After activating the instruments, flat field images were taken to account for limitations in the imaging apparatus, such as dusty lenses, sensor noise, and vignetting. This step is crucial for image reduction. Then, the telescope was focused on a reference star with an apparent magnitude of 4-5. After this, the telescope was slewed to the asteroid's position using the RA and DEC predicted by JPL Horizons. Next, the location of the asteroid within the frame was roughly determined by comparing the image to the star map generated prior to the observation using the Tapir package. At this point, three sequences of images were taken, each ten minutes apart. In each sequence, a set of dark images and a set of light images were captured.

2.2. *Image Reduction*

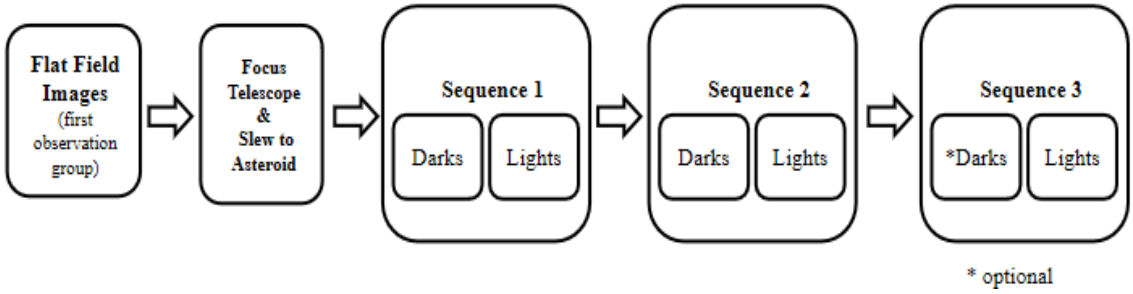

Figure 1: Observation Process

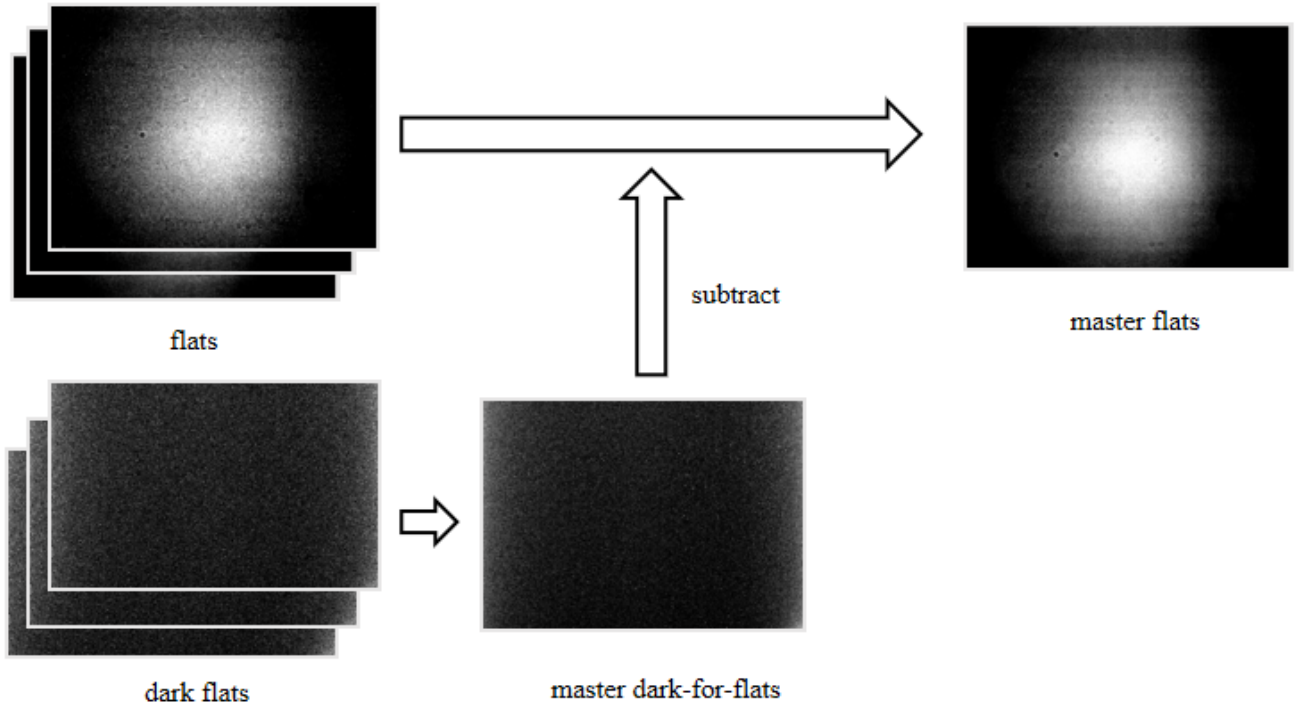

Figure 2: Image Processing: Building Master Flat

In the image processing stage, AstroImageJ was used to mitigate noise and imperfections in the imaging setup by subtracting the master flat and darks from the light series. For instance, the effects of vignetting and dust particles within the telescope were reduced. To make the asteroid more visible, signal was strengthened by stabilizing, aligning, and compiling each sequence of light images into a single image. Finally, to confirm the position of the asteroid for each observation, the three processed images from each night were aligned and then blinked forward so that the asteroid visibly moves on the screen.

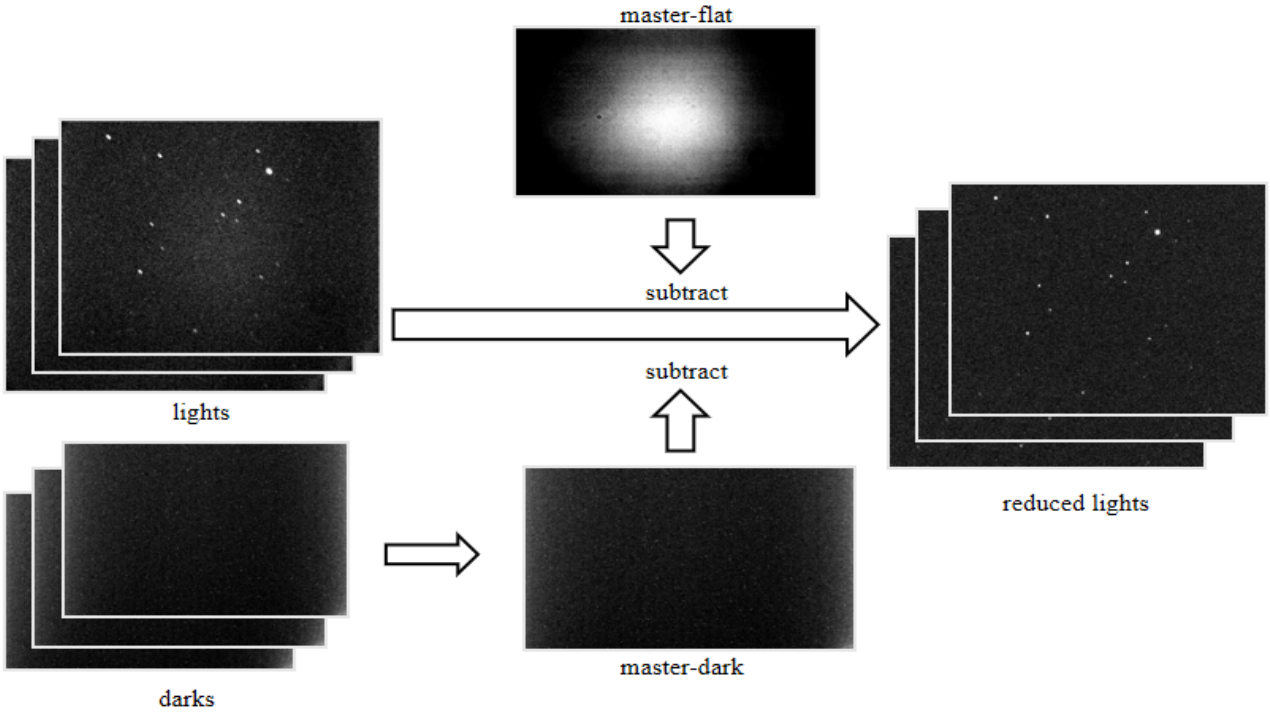

Figure 3: Image Processing: Getting Reduced Images

2.3. *Astrometry*

The goal of astrometry is to obtain the RA and DEC of the asteroid for each of the three nights of observations. To achieve this, the Least-Squares Plate Reduction (LSPR) method was applied using each image and the USNO-B Catalog. To do this, the second processed image taken for each night was uploaded to nova.astrometry.net. The site utilizes the LSPR method to compute the six plate constants and their uncertainties, where it uses a least squares regression fit. The site generates a new FITS file that contains the RA and DEC information for the asteroid. Additionally, it creates a corr.fits file, which includes both the measured RA and DEC value and the catalog RA and DEC value. These values will be important for uncertainty determination. Once downloading these files, RA and DEC was converted from degrees to hours minutes seconds and sexagesimal units respectively for use as inputs in orbit determination.

2.4. *Photometry*

The goal of photometry is to determine the apparent magnitude of the asteroid. To achieve this, five reference stars were selected from the images that are also included in the APASS catalog in SAOImageDS9. After identifying the relationship between the signals from AstroImageJ and the apparent magnitudes in the APASS catalog, the apparent magnitude of the asteroid was determined based on its own signal.

2.5. *Results and Uncertainty*

To determine the uncertainty in astrometry, the data in the corr.fits file from nova.astrometry was analyzed. By computing the Root Mean Square (RMS) of the differences between the expected and measured values for RA and DEC, the uncertainty can be calculated.

Table 3: Observation Results

Time of Observation (JD)	RA	RA Error	DEC	DEC Error	Apparent Magnitude
2459785.59022	14 58 30.37	1.48×10^{-4}	-15 39 26.5	1.10×10^{-1}	13.7
2459785.59784	14 58 30.15	1.48×10^{-4}	-15 39 21.9	1.01×10^{-4}	14.6
2459785.60339	14 58 30.00	2.20×10^{-4}	-15 39 18.4	1.97×10^{-4}	14.6
2459789.63181	14 57 01.35	7.90×10^{-5}	-15 00 10.5	1.02×10^{-4}	14.7
2459789.63878	14 57 01.24	8.75×10^{-2}	-15 00 06.4	7.74×10^{-5}	14.6
2459789.64595	14 57 01.07	1.04×10^{-4}	-15 00 02.3	1.19×10^{-4}	14.5
2460495.47845	14 55 45.35	9.51×10^{-5}	-13 38 47.1	1.26×10^{-4}	14.7
2460495.48909	14 55 45.36	1.40×10^{-4}	-13 38 42.6	1.30×10^{-4}	14.6

3. ORBIT DETERMINATION

An orbit is completely determined by the position and velocity vectors of the object. Thus, to find the orbital elements, the position and velocity vectors must be extracted from the observations.

It should be noted that as Gaussian units are used, $\mu = GM_\odot = 1$. Vectors will be denoted as $\vec{V}$, their magnitudes will be denoted as V, and their unit vectors will be $\hat{V} = \vec{V}/V$.

3.1. *Methods*

There are many ways to extract the orbital parameters from measurements. The most commonly used method for orbital determination is Gauss's method. Gauss's method begins with a first guess for the position and velocity vectors using Kepler's Laws. These guesses are then updated iteratively until their change is under a convergence interval. At this point, the orbital elements are determined from the vectors.

3.1.1. *Gauss's Method*

Gauss's method was used to solve for the orbit of the asteroid. Gauss's method uses 3 nights of data, which can be modeled by 3 different sun to asteroid vectors, $\vec{r_1}, \vec{r_2}, \vec{r_3}$. Then, $\vec{r_2}$ can be expressed as a linear combination of the two other vectors, because they are all co-planar.

$$\vec{r_2} = a_1\vec{r_1} + a_3\vec{r_3}$$

A first guess of a_1 and a_3 was found by using Kepler's second law and approximating the orbital areas as triangles. Let t_1, t_2, t_3 be the times of the observations respectively. Then the time of the first observation with respect to the second is $\tau_1 = t_1 - t_2$. Similarly, the time of the third observation with respect to the second is $\tau_3 = t_3 - t_2$. From Kepler's second law, $A \propto t$. The approximate area of the orbit during those times are $\frac{\vec{r_2}\times\vec{r_1}}{2}$ and $\frac{\vec{r_2}\times\vec{r_3}}{2}$ respectively. Note that the area and the times are both negative for the first slice. The area between the first and third observation is $\frac{\vec{r_1}\times\vec{r_3}}{2}$ and is proportional to time $\tau_3 - \tau_1$. Then,

$$\frac{\tau_1}{\tau_3 - \tau_1} = \frac{\vec{r_2}\times\vec{r_1}}{\vec{r_1}\times\vec{r_3}} = \frac{(a_1\vec{r_1} + a_3\vec{r_3})\times\vec{r_1}}{\vec{r_1}\times\vec{r_3}} = \frac{0 + a_3\vec{r_3}\times\vec{r_1}}{\vec{r_1}\times\vec{r_3}} = -a_3.$$

Doing this process again,

$$a_1 = \frac{\tau_3}{\tau_3 - \tau_1}$$
$$a_3 = \frac{-\tau_1}{\tau_3 - \tau_1}$$

However, because the asteroid is viewed from Earth, only the direction of the asteroid from the earth, $\hat{\rho}$, is seen. The magnitude of $\vec{\rho}$ is not known. In terms of RA and DEC, this unit vector is

$$\hat{\rho} = \begin{bmatrix} \cos(\alpha)\cos(\delta) \\ \sin(\alpha)\cos(\delta) \\ \sin(\delta) \end{bmatrix}$$

Now, the earth to asteroid vector $\vec{\rho}$ can be written as a combination of the earth to sun vector $\vec{R}$ and the sun to asteroid vector $\vec{r}$.

$$\rho\hat{\rho} = \vec{r} + \vec{R}.$$

All the $\vec{r}$ vectors can be written in terms of ρ, which is unknown, as well as $\hat{\rho}$, which is known from the observations. Finally, the $\vec{R}$ vector for each night is acquired from JPL Horizons.

$$\begin{aligned} \vec{r_1} &= \rho_1\hat{\rho}_1 - \vec{R}_1 \\ \vec{r_2} &= \rho_2\hat{\rho}_2 - \vec{R}_2 \\ \vec{r_3} &= \rho_3\hat{\rho}_3 - \vec{R}_3 \end{aligned} \tag{1}$$

Substituting it back into the linear combination for r_2 gets

$$a_1\rho_1\hat{\rho}_1 - \rho_2\hat{\rho}_2 + a_3\rho_3\hat{\rho}_3 = a_1\vec{R_1} - R_2 + a_3\vec{R}_3$$

which is just a system of linear equations in terms of $\rho_{1,2,3}$. This can be solved using Cramer's rule.

$$\rho_1 = \frac{\hat{\rho_2} \cdot (\hat{\rho_3} \times (a_1\vec{R_1} - R_2 + a_3\vec{R_3}))}{a_1\hat{\rho_1} \cdot (\rho_2 \times \rho_3)}$$
$$\rho_2 = \frac{\hat{\rho_3} \cdot (\hat{\rho_1} \times (a_1\vec{R_1} - R_2 + a_3\vec{R_3}))}{-\hat{\rho_1} \cdot (\rho_2 \times \rho_3)}$$
$$\rho_3 = \frac{\hat{\rho_1} \cdot (\hat{\rho_2} \times (a_1\vec{R_1} - R_2 + a_3\vec{R_3}))}{a_3\hat{\rho_1} \cdot (\rho_2 \times \rho_3)}$$

After solving for $\vec{\rho}$, it can be plugged back in to solve for the $\vec{r}$ vectors.

To find the initial guess for $\dot{\vec{r_2}}$, an average velocity is taken to approximate it from nights 1 to 3.

$$\dot{\vec{r_2}} = \vec{v_2} \approx \frac{\vec{r_3} - \vec{r_1}}{\tau_3 - \tau_1}$$

Then, a Taylor series can be constructed from the $\vec{r_2}$ and $\vec{v_2}$ values, to better approximate $\vec{r_1}$ and $\vec{r_3}$, which will help get better guesses for a_1 and a_3.

The Taylor series follows the form of

$$\vec{r}(\tau) = \vec{r}_2 + \vec{v}_2\tau + \ddot{\vec{r}}_2 \frac{\tau^2}{2!} + \dddot{\vec{r}}_2 \frac{\tau^3}{3!} + ...$$

The second order term can be found through Newton's Law of Gravitation, which is

$$\ddot{\vec{r}}_2 = -\frac{1}{r_2^3}\vec{r_2}.$$

The third order term can be found by taking the derivative of this.

$$\dddot{\vec{r}}_2 = \frac{3(\vec{r_2} \cdot \vec{v_2})}{r_2^4}\vec{r_2} - \frac{1}{r_2^3}\vec{v_2}.$$

Similarly all the subsequent orders can be found by taking derivatives of the original equation and plugging in initial conditions. These derivatives are all split up into a basis, written as a combination of terms of $\vec{r}_2$ and $\vec{v}_2$. The Taylor series can be written in the basis as follows

$$\vec{r}(\tau) = f(\tau)\vec{r}_2 + g(\tau)\vec{v}_2$$

where to fourth order,

$$f(\tau) = 1 - \frac{\tau^2}{2r_2^3} + \frac{(\vec{r_2} \cdot \vec{v_2})\tau^3}{2r_2^5} + \frac{\tau^4}{24r_2^3}\left(3\left(\frac{v_2^2}{r_2^2} - \frac{1}{r_2^3}\right) - 15\left(\frac{(\vec{r_2} \cdot \vec{v_2})}{r_2^2}\right)^2 + \frac{1}{r_2^3}\right)$$

$$g(\tau) = \tau - \frac{\tau^3}{6r_2^3} + \frac{(\vec{r_2} \cdot \vec{v_2})\tau^4}{4r_2^5}.$$

Define $f_1 = f(\tau_1), f_3 = f(\tau_3)$ and similarly for g. Then,

$$\vec{r_1} = f_1\vec{r_2} + g_1\vec{v_2}$$

$$\vec{r_3} = f_3\vec{r_2} + g_3\vec{v_2}$$

and by definition

$$a_1\vec{r_1} + a_3\vec{r_3} = \vec{r_2}.$$

For this condition to be true,

$$a_1 = \frac{g_3}{f_1 g_3 - f_3 g_1}$$

and

$$a_3 = \frac{-g_1}{f_1 g_3 - f_3 g_1}.$$

A better approximation for the velocity $\vec{v_2}$ can also be obtained, in terms of the f and g functions and the new $\vec{r_1}$ and $\vec{r_3}$.

$$\vec{v_2} = \frac{f_3\vec{r_1} - f_1\vec{r_3}}{f_3 g_1 - g_3 f_1}.$$

The new values are updated and this process is iterated until the convergence interval is below a certain threshold. After the initial $\vec{r_1}$, $\vec{r_2}$, and $\vec{r_3}$ vectors are found, a correction can also be introduced for light travel time, updating $t_i' = t_i - \frac{r_i}{c}$ in each iteration.

3.1.2. *Orbital Element Determination*

After extracting $\vec{r}$ and $\vec{v} = \dot{\vec{r}}$ values from the data, the orbital elements were found. It should be noted that as the RA and DEC were found in the equatorial plane, it had to be transformed using rotational matrices to the ecliptic plane.

The first element, the inclination, can be found by finding the specific angular momentum vector $\vec{l} = \vec{r} \times \vec{v}$. The inclination is just the angle the angular momentum vector makes with the z axis, which is just

$$i = \arccos\left(\frac{\vec{l} \times \hat{z}}{l}\right).$$

To find the longitude of the ascending node, the vector for the line of nodes is required. This is the part of the orbit where the ellipse intersects the $x - y$ plane. The cross product of any vector with the angular momentum vector always yields a vector in the orbital plane. Any vector that is crossed with the $\hat{z}$ vector yields a vector in the $x - y$ plane. Thus, $\vec{n} = \vec{l} \times \hat{n}$ is the place where the

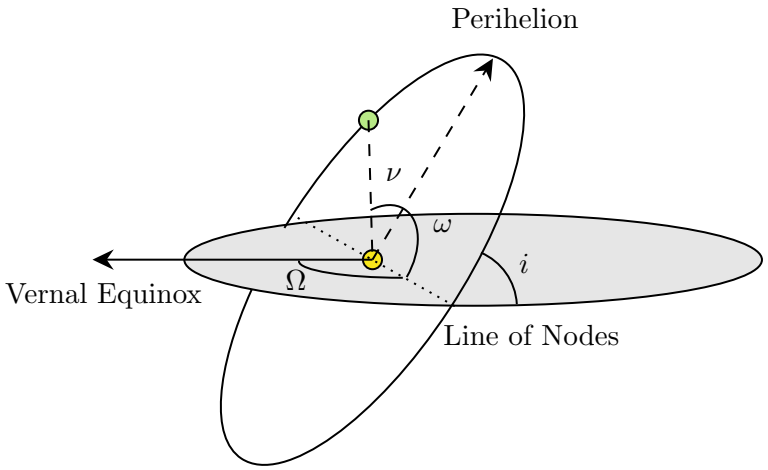

Figure 4: 4 Orbital Elements

orbit intersects the plane, i.e. the line of the ascending node. The function atan2 is used to avoid sign ambiguity.

$$\Omega = \text{atan2}\left(\vec{n} \cdot \hat{y}, \vec{n} \cdot \hat{x}\right) \mod 2\pi$$

atan2(y, x) returns the phase or argument of the complex number $x + iy$. This is returned between $-\pi$ and π so in order to get the angle in between 0 and 2π, a modulus of 2π is taken.

The semi-major axis and eccentricity of the orbit can found from the specific energy of the orbit. In Gaussian units,

$$E = \frac{1}{2}(v)^2 - \frac{1}{r}.$$

By the virial theorem, $E = -\frac{1}{2a}$ so

$$a = -\frac{1}{2E}.$$

The formula for the eccentricity of the orbit is

$$e = \sqrt{1 + 2E \cdot l^2}.$$

From Kepler's laws, it is known that the path of an orbit takes the form of an ellipse, with the equation

$$r = \frac{a(1 - e^2)}{1 + e\cos(\nu)}$$

where ν is the true anomaly. Rearranging,

$$\cos(\nu) = \frac{a}{re}(1-e^2) - \frac{1}{e}.$$

Since ν has a range between 0 and 2π there is sign ambiguity. This can be avoided by taking the derivative with respect to ν which yields

$$\dot{r} = \frac{a(1-e^2)}{(1+e\cos(\nu))^2} \cdot e\sin(\nu)\dot{\nu} = \frac{r^2}{a(1-e^2)} \cdot e\sin(\nu)\dot{\nu}$$

where

$$\dot{r} = \frac{d}{dt}(\vec{r}\cdot\hat{r}) = \dot{\vec{r}}\cdot\hat{r} + \vec{r}\cdot\dot{\theta}\hat{\theta} = \vec{v}\cdot\hat{r} + 0 = \vec{v}\cdot\hat{r}$$

and by angular momentum conservation

$$\dot{\nu} = l/r^2.$$

Plugging this back in, and rearranging

$$\sin(\nu) = \frac{a(1-e^2)(\vec{v}\cdot\hat{r})}{le}$$

Then,

$$\nu = \text{atan2}\left(\frac{a(1-e^2)(\vec{v}\cdot\hat{r})}{le}, \frac{a}{re}(1-e^2) - \frac{1}{e}\right) \mod 2\pi.$$

Defining $u = \omega + \nu$, the argument of perihelion plus the true anomaly, a new relationship can be obtained as this is just the angle between $\vec{r}$ and $\vec{n}$, which can be extracted using dot products and cross products.

$$\cos(u) = \frac{\vec{r}\cdot\vec{n}}{rn}.$$

$$\sin(u) = \left|\frac{\vec{r}\times\vec{n}}{rn}\right|.$$

Then,

$$\omega = \text{atan2}\left(\frac{\vec{r}\cdot\vec{n}}{rn}, \left|\frac{\vec{r}\times\vec{n}}{rn}\right|\right) - \nu \mod 2\pi.$$

The six orbital elements have been recovered from the position and velocity vectors.

3.1.3. *Monte-Carlo Error Determination*

Using the standard deviations for the RA and DEC acquired from the astrometry, the Method of Gauss was run to determine the orbital elements while taking into account the confidence in the RA and DEC for each night. In order to to this, random values for the RA and DEC for each night are calculated, centered around their mean and varied by their standard deviation. Then, the orbital elements are calculated and stored. This is repeated for 1,000,000 samples to get the mean and the Standard Deviation of the Mean (SDOM) values for the six orbital elements.

3.1.4. *Ephemeris Generation*

The Ephemeris has an input of time and an output of the RA and DEC in Equatorial Coordinates. In order to reverse engineer the time, the mean anomaly must be used, which is defined as

$$\frac{M}{2\pi} = \frac{t-T}{P} = \frac{\delta t}{P}$$

where T is the time of perihelion and P is the period of the orbit. To convert back to eccentric anomaly, use

$$E - e\sin(E) = M.$$

This equation cannot be solved exactly so the Newton-Raphson Method is used to find the eccentric anomaly as a function of time.

$$\vec{r} = \begin{bmatrix} a\cos(E) - ae \\ a\sqrt{1-e^2}\sin(E) \\ 0 \end{bmatrix}$$

Then, the heliocentric $\vec{r}$ vector is found using the orbital elements. First, $\vec{r}$ is rotated about z by the argument of perihelion ω, then rotated about x by the inclination i, and then finally about z again by the longitude of the ascending node Ω. The ecliptic earth to sun vector $\vec{R}$ is added to this vector to get the $\vec{\rho}$ vector. This is then rotated from the ecliptic plane to the equatorial plane using

a rotation matrix. Then, the components of $\hat{\rho}$ are combined to find the RA and DEC.

$$\hat{\rho} = \begin{bmatrix} \cos(\alpha)\cos(\delta) \\ \sin(\alpha)\cos(\delta) \\ \sin(\delta) \end{bmatrix}$$

$$\delta = \arcsin \hat{\rho} \cdot \hat{z}$$

$$\alpha = \text{atan2}(\hat{\rho} \cdot \hat{y}, \hat{\rho} \cdot x) \mod 2\pi$$

3.1.5. *Self-Consistency Check*

In order to verify methodology, a self-consistency check was used where the orbital elements calculated were used in an ephemeris to calculate the RA and DEC for the third observation. The third observation was 9 days after the second observation and 13 days after the first observation.

3.2. *Results*

Figure 5: Histogram of Orbital Elements, N = 1,000,000

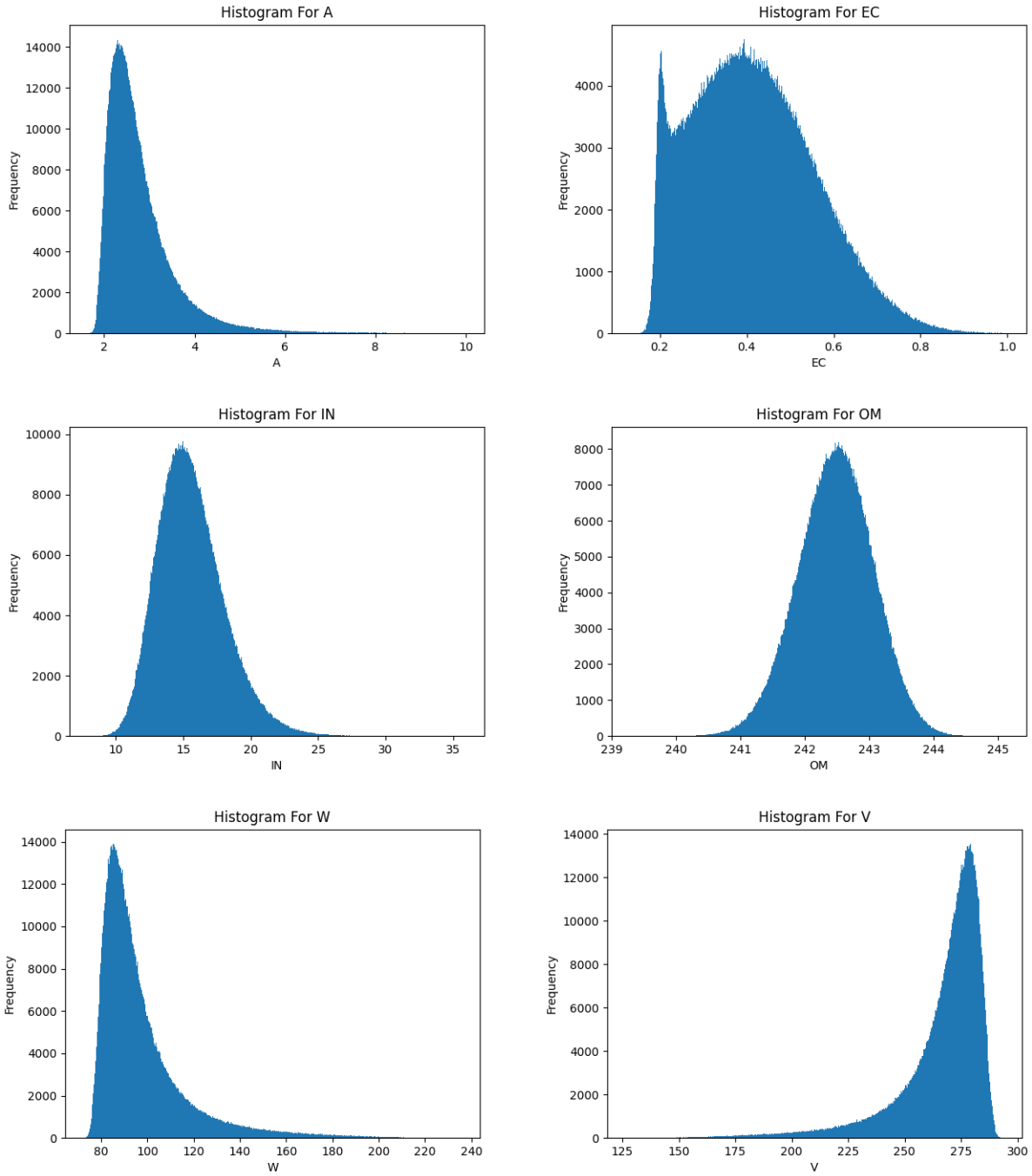

Table 4: Orbital Elements and Uncertainties

OD Element	Value (AU, deg)	±SDOM	JPL Values	% Dif
a Semi-Major Axis	2.5995	±0.005	2.6134	0.53%
e Eccentricity	0.4056	±0.0004	0.4095	0.97%
i Inclination	15.344	±0.008	15.293	0.33%
Ω Longitude of Ascending Node	242.492	±0.002	242.497	.002%
ω Argument of Perihelion	91.76	±0.06	91.46	0.32%
ν True Anomaly	272.31	±0.06	272.62	0.11%

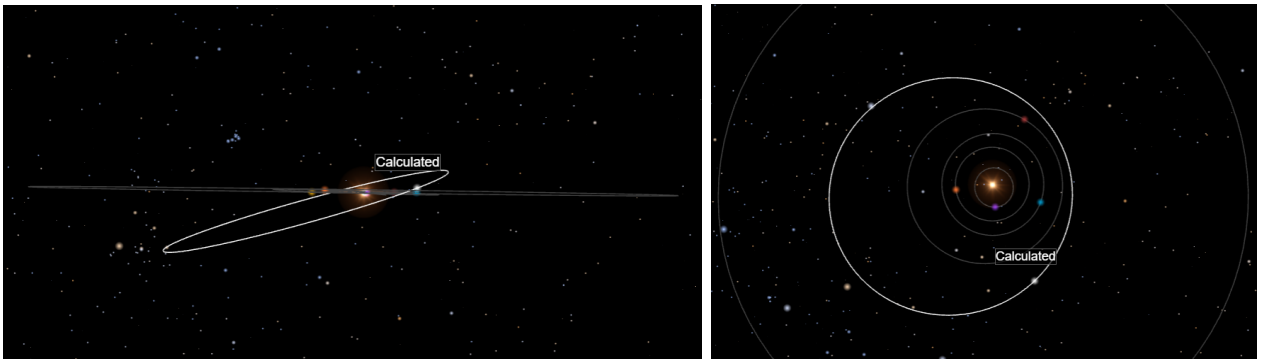

Figure 6: Side and Top Views of Orbits

4. DISCUSSION

Results were the same between teammates after rounding to appropriate significant figures for all orbital elements. The difference between the calculated results and JPL's ephemeris was less than 1% for all orbital elements. Outside of eccentricity, orbital elements varied by less than 0.55% versus JPL. The RA of the asteroid varied by 0.01 seconds and the DEC by 0.0 arcseconds on the first and third observations between telescope observations and JPL. The second observation varied by 0.03 seconds and 0.5 arcseconds in RA and DEC respectively. It should be noted that most of the standard deviations are higher than the percent difference between calculated and JPL values, which means that the JPL ephemeris' orbital elements are contained within the margin of error in the study.

In the self consistency check, the obtained ephemeris RA from the orbital elements was 1.64 minutes above the measured RA from the third night, while the DEC was 2.85 arcminutes under measured. This suggests a successful implementation of the methods used, though it also hints at some error in RA and DEC values found from observations.

The most notable source of error during orbit determination was that the Pohl Observatory telescope used had notable wobble. This telescope was used on the first two nights. The wobble led to clear shift in apparent position of stars and asteroids in images taken with as shown by stars turning into lines as exposure increased. By extension, this suggests slight but relevant variability in calculated RA and DEC on the first two nights. A notable gap between measured RA and DEC is seen when compared to JPL on night two, supporting this conclusion. Even small deviations in RA and DEC led to shifts in orbital elements, so this uncertainty is notable (figure 5). The Monte Carlo simulation used a standard deviation of 10^{-4} radians in RA and DEC values and led to large shifts in orbital elements. One other factor which may have affected results is the variation in times between observations. Four days passed between the first and second observation taken, but nine days passed between second and third observations. This variation could cause some error when applying the Method of Gauss. Possible improvements in procedure could include using a single telescope, keeping time between observations constant, and using a telescope with reduced wobble.

5. REFLECTION

The experience of working on this project was both challenging and rewarding. Our team collaborated effectively. We communicated regularly and helped each other out when we encountered problems. We also set interim deadlines, switched roles as necessary, and all went through and edited everything to reach a final draft we were satisfied with. We collaborated using overleaf.

We divided the tasks based on individual strengths and preferences: Jean focused on astrometry and our MPC report, I focused on the discussion, programming, and editing, and Sour focused on theoretical methods and results. I particularly enjoyed the programming, from creating pretty Monte Carlo histograms to animating the Method of Gauss in action. Jean particularly enjoyed observations and astrometry, taking us from an expansive night sky to a clear image of our asteroid. Sour enjoyed

"mathing": reverse engineering the vector that brought us D values and flying solo without the cookbooks (and occassionally getting cooked because of it, he wants me to add. Debugging with him took a little while, but I wouldn't trade the bonding experience for the world.) He also frequently did the impossible with Latex.

Ultimately, our team played to our strengths and really enjoyed the project. On our first day, we worked together to draft a creatively written piece on Norse Mythology and Hela for our asteroid proposal. Five short weeks later, we, like Hela, have certainly come a far way together.

6. ACKNOWLEDGEMENTS

Thank you to all the incredible students we've met at SSP, who have created a collaborative community and helped each other make it through this project. Thank you to our TAs for answering our questions whenever we came to them. Thank you to Dr. C, Dr. D, and Dr. M, for teaching us all we needed for this project and more in six short weeks. We've learned an incredible amount here thanks to you. Thank you to Dr. Ice for keeping the program running and injecting in fun and humor, from dinner announcements to field trips and everything in between. In short, thank you SSP. We'll always remember this experience fondly.

REFERENCES

[1]Home page - iasc: International astronomical search collaboration, 2007.

[2]Roger R Bate, Donald D Mueller, Jerry E White, and William W Saylor. *Fundamentals of astrodynamics*. Dover Publications, Inc, 1971.

[3]Dan L Boulet. *Methods of Orbit Determination for the Microcomputer*. Willmann-Bell, 1991.

[4]John M A Danby. *Fundamentals of celestial mechanics*. Willmann-Bell, Inc., 1992.

[5]Carl Friedrich Gauss. *Theory of the Motion of the Heavenly Bodies Moving about the Sun in Conic Sections*. Dover Publications, Inc., 1963.

[6]J.B. Tatum. *Celestial Mechanics*. 2008.